

Minimizing Voltage Tuning for Enhanced High Field Energy Storage

Geoff L. Brennecke, Kelsey E. Meyer*, Yu Hong Jeon**, David I. Shahin***, Harlan J. Brown-Shaklee, Brady Gibbons**, and Jon F. Ihlefeld

Sandia National Laboratories, Albuquerque, NM 87185-1411 USA

Fax: 81-505-844-9781, e-mail: glbrenn@sandia.gov

*New Mexico Institute of Mining and Technology, Socorro, NM USA

**Oregon State University, Corvallis, OR USA

***Missouri University of Science and Technology, Rolla, MO USA

Use of high-permittivity ceramics for capacitive energy storage is plagued by the reduction in permittivity with increased applied electric field, a phenomenon known as voltage tuning. We present here our efforts to design in minimal tuning in Bi-modified BaTiO₃-based ceramics through careful control of cation distribution and microstructure development. With appropriate processing, dense ceramics have been formed which maintain permittivity values >1500 at fields up to 100kV/cm and voltages up to 10kV, resulting in enhanced stored electrostatic energy over similar commercial high-voltage BST-based capacitors. Further, these materials maintain their nearly-linear voltage response across broad temperature ranges. Combined with improved processing for greater reliability, this approach offers a promising alternative for high energy density high voltage capacitors for load leveling and rapid-response supplements to mid-to-large scale backup power systems.

This work was supported by the Office of Electricity's Energy Storage program managed by Dr. Imre Gyuk. Sandia National Laboratories is a multi-program laboratory managed and operated by Sandia Corporation, a wholly owned subsidiary of Lockheed Martin Corporation, for the U.S. Department of Energy's National Nuclear Security Administration under contract DE-AC04-94AL85000.

Key words: Capacitor, voltage tuning, breakdown, storage

1. INTRODUCTION

Capacitors are used for a great number of applications, and each application requires optimization of the materials behavior most appropriate to the end use. Most capacitor applications desire large capacitance density under target operating conditions, but many applications such as filtering and decoupling typically involve voltage swings which are relatively small compared to the ultimate breakdown voltage of the capacitor. Further, for such applications, the nonlinear permittivity response of typical high-permittivity ferroelectric-based materials is not necessarily a concern; while a decrease in permittivity with increasing applied field may not be desirable for such applications, it is not a critical design parameter. In fact, many applications take advantage of this voltage tuning in order to adjust circuit parameters through the use of a dc bias. For energy storage applications—or, more appropriately when discussing electrostatic mechanisms, power applications—however, voltage tuning greatly reduces the available storage because the energy (U) stored in a capacitor is represented by the equation:

$$U = \frac{1}{2} CV^2$$

or, more appropriately for non-linear materials:

$$U = \int_0^{E_{max}} \epsilon_0 \epsilon_r(E) EdE$$

where C represents capacitance, V is applied voltage, E is applied electric field, ϵ_0 is the permittivity of free space, and $\epsilon_r(E)$ is the field-dependent relative permittivity. This directly highlights the importance of maintaining a large permittivity at high fields if stored energy is to be maximized but of course also assumes that these large fields can be accessed prior to dielectric breakdown. It is well known that dielectric breakdown follows critical flaw Weibull statistics, so the challenge of actually fabricating a high-breakdown-strength (and therefore high energy density) capacitor becomes increasingly more challenging as either the desired energy or desired operating voltage increases. For example, we have previously fabricated PZT-based thin films with energy densities greater than 20 J/cm³ (Figure 1),¹ but such films are only useful for operating voltages ~150V or less and provide <1mJ of total stored energy. Currently, applications requiring the rapid discharge available from electrostatic capacitors, >1J of energy, and/or operating voltages >1kV are nearly forced to use polymer dielectrics. Clearly, in order for ceramic capacitors to compete for high-energy applications, significant advances are required. Our group is presently working on two aspects of this problem: maintaining high permittivity values under large fields (i.e., minimizing voltage tuning) and fabricating large-area high-breakdown-strength capacitors that can reliably operate at high voltages (1-20kV). The present discussion will focus on our work towards minimizing voltage tuning at high fields.

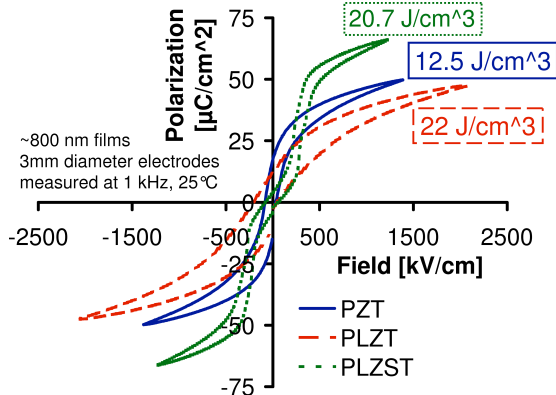


Figure 1 – PZT-based thin films have been fabricated with energy densities in excess of $20\text{J}/\text{cm}^3$, but the same small active volumes that enable such high-field operation also limit operating voltages to (at most) 150–200V and total stored energies to mJ levels (from Sigman *et al.*¹).

Groups at Oregon State University^{2,3} the Pennsylvania State University,⁴ and others^{5,6} have recently reported encouraging results from BaTiO_3 -based ceramics modified with a variety of Bi-based $\text{Bi}(\text{M})\text{O}_3$ materials where M can represent a single or multiple small B-site cations (e.g., Sc , $\text{Zn}+\text{Ti}$, $\text{Mg}+\text{Ti}$, etc.) whose solid-solutions show nearly-linear polarization-field response out to rather large fields. Significant work has also been carried out on similar solid solutions with a Pb-based end member.^{7–10} A common theme among these materials is that the Bi-based end member is (often) unstable as a stand-alone perovskite material under ambient pressures, but that mixing with a stable perovskite such as BaTiO_3 or PbZrO_3 forms a stable perovskite solid solution that exhibits relaxor-like behavior over relatively broad temperature ranges. Inspired by this work, we are investigating the structural/microstructural origin(s) of the minimal field-saturating polarization behavior observed in these materials, particularly how they compare to $(\text{Pb},\text{La})(\text{Zr},\text{Ti})\text{O}_3$ and related high-permittivity materials that also exhibit minimal saturation under large electric fields.

2. EXPERIMENTAL PROCEDURES

All samples discussed here were produced using standard mixed-oxide processing techniques from simple oxide or carbonate precursors. Batched powders were ball milled for 6hrs in ethanol for thorough mixing, dried overnight, calcined at temperatures ranging from 820 – 1100°C for 2 – 6 hours, and then ball milled again. During the final hour of the second ball milling step, a small amount of PVB solution (corresponding to ~3wt% PVB relative to the solids) was added to serve as a binder during subsequent processing. The dried powders were ground in a mortar and pestle to thoroughly mix in any unbound PVB and were pressed into pellets ~1mm thick and ~13mm in diameter under uniaxial pressure of ~100MPa using a Carver press. Typical green densities (as determined by simple geometric measurements) ranged from 3.3 – 3.7g/cm³, corresponding—depending upon exact composition—to between 50 and 60% of

theoretical density, with the theoretical density for each individual composition calculated from the d-spacing values obtained by X-ray diffraction (XRD). Green pellets were buried in a loose powder of their own composition and then sintered in covered Al_2O_3 crucibles. Sintering runs consisted of a slow 2°C/min ramp to 400°C for binder removal followed by a slightly faster (3–5°C/min) ramp up to the final sintering temperature, which varied from 1000 – 1390°C. Hold times at the maximum sintering temperature ranged from 0 – 12 hours, and cooling rates varied from an uncontrolled passive furnace-cool to a controlled maximum cooling rate of 2°C/min. Sintered samples varied in density from 88–99% theoretical; samples whose dielectric data are discussed here were all >97% theoretical density as determined by the (Archimedes) fluid displacement technique using (boiling) water as the displacement fluid.

Sintered samples were polished to a 1μm surface finish and each face was coated with a Ag-based screen printing ink which was then fired on at 400°C, 1hr. Small signal dielectric data were collected using an HP4284A impedance analyzer with scans from 20Hz – 100kHz with an oscillator amplitude of 1V. Similar measurements of the small-signal permittivity on top of a dc bias of up to 3kV were performed on the same HP4284A but with a custom high-voltage blocking circuit in-line. A Precision Workstation from Radian Technologies (Albuquerque, NM) attached to a 10kV Trek amplifier was used to collect polarization vs. electric field data at 0.1, 1, and 10Hz. For high voltage measurements, samples were immersed in Fluorinert FC-40.

A Zeiss Supra 55VP Field Emitter Gun Scanning Electron Microscope (FEG SEM) was used for microstructural imaging and analysis. XRD on both powder and pellet samples was carried out on several instruments, including a Rigaku DMax, Philips X'Pert, and Philips MRD, all with copper K_α radiation in standard Bragg-Brentano geometry.

3. RESULTS AND DISCUSSION

We focus here on three specific compositions: $80\text{BaTiO}_3\text{-}20\text{BiScO}_3$, $80\text{BaTiO}_3\text{-}20\text{Bi}(\text{Zn}_{0.33}\text{Ti}_{0.67})\text{O}_3$, and $90\text{BaTiO}_3\text{-}10\text{Bi}(\text{Zn}_{0.33}\text{Ti}_{0.67})\text{O}_3$, hereafter referred to as 80BT-20BS, 80BT-20BZT, and 90BT-10BZT, respectively. Figure 2 summarizes the XRD results discussed below. Regardless of calcination conditions, 80BT-20BS powders always contained extraneous peaks that were apparently associated with minor residual Bi_2O_3 and $\text{Bi}_4\text{Ti}_3\text{O}_{12}$. SEM analysis using backscattered electron imaging and energy dispersive spectroscopy (EDS) mapping (not shown here) confirmed the presence of discrete high-z particles consistent with Bi_2O_3 and $\text{Bi}_4\text{Ti}_3\text{O}_{12}$. Following sintering at 1390°C for 6 hours, however, the only diffraction peaks observed could be assigned to the perovskite phase. BT-BZT compositions formed single-phase perovskite powders after 4 hours at 950°C. The diffraction patterns were all quite similar to cubic BaTiO_3 , (shown at the bottom of Figure 2 for reference). Refinement of the diffraction pattern from calcined 0.8BT-0.2BZT, for example, determined a cubic unit cell with a lattice parameter of 4.009(1)Å.

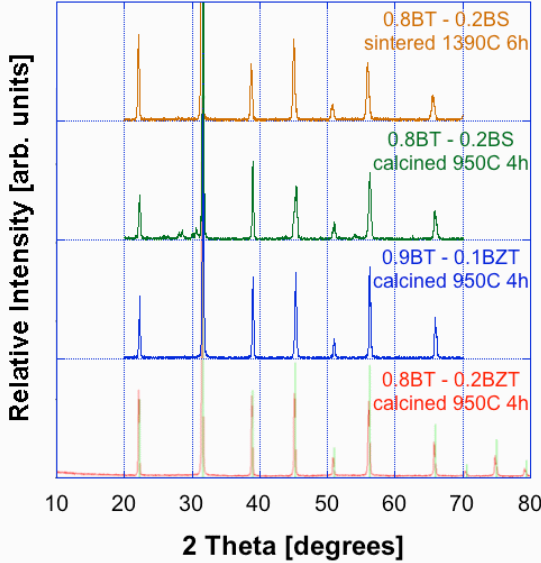


Figure 2 – XRD analysis showed that BT-BZT powders formed single phase perovskite after calcination (shown here, 950°C 4h), but calcined BT-BS powders contained residual Bi_2O_3 and $\text{Bi}_4\text{Ti}_3\text{O}_12$ phases even after calcination at 1100°C for 12h (not shown) which were finally consumed during sintering. A reference diffraction pattern for cubic BaTiO_3 is shown as the sharp green lines on the bottom of the plot for comparison.

Under the sintering conditions investigated for (1-x)BT-xBZT samples (relatively slow ramp rates in air with hold temperatures between 1000-1200°C), neither composition showed a strong relationship between sintering time and either relative density or average grain size. All sintered samples exhibited broad grain size distributions. BZT content strongly influenced the sintering of (1-x)BT-xBZT samples. 0.9BT-0.1BZT specimens maintained significantly finer grain sizes than their 0.8BT-BZT counterparts sintered under identical conditions, though final sintered relative density values were similar. For example, when sintered in air at 1180°C for 12 hours with a controlled maximum cooling rate of 5°C/min, both 0.9BT-0.1BZT and 0.8BT-0.2BZT samples achieved >98% relative density values, but the average grain size of the 0.8BT-0.2BZT sample ($8.4 \pm 5.2 \mu\text{m}$) was nearly 10x the average grain size of the 0.9BT-0.1BZT sample ($1.1 \pm 0.7 \mu\text{m}$). Figure 3 illustrates this with representative images of these specimens. More detailed sintering studies are currently underway for these compositions and several others.

Pure BaTiO_3 is the prototype ferroelectric material with a first-order phase transition between cubic and tetragonal phases at the Curie point. BZT additions to BT induce a relaxor-like dielectric response and a broadening of the temperature-dependent permittivity that accompanies a ‘smearing-out’ of the structural phase transition. The structure of this lower-temperature phase remains tetragonal for 10% additions of BZT, but 20% BZT additions result in a gradual rhombohedral–cubic transition.³ The temperature and frequency dependence of the relative permittivity and tangent delta values measured for our 0.9BT-0.1BT and 0.8BT-0.2BZT samples can be seen in Figure 4.

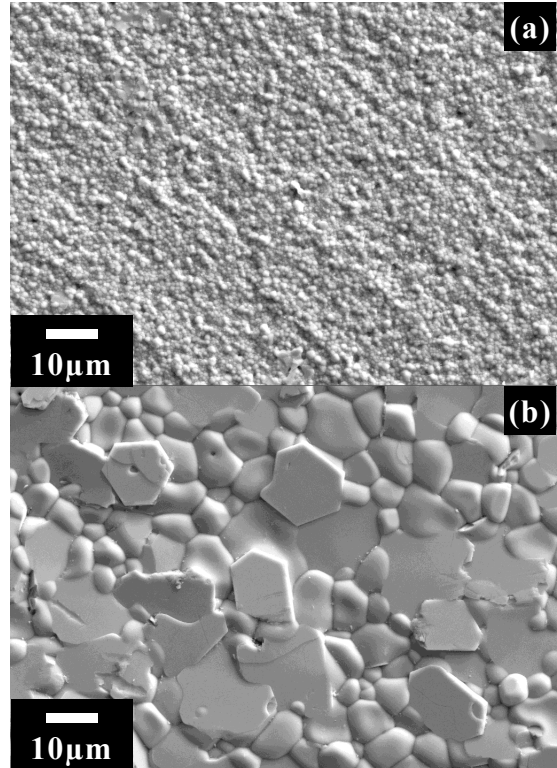


Figure 3 – Representative surface microstructures of (a) 0.9BT-0.1BZT and (b) 0.8BT-0.2BZT samples sintered at 1180°C, 12 hours with a controlled maximum 5°C/min cooling rate.

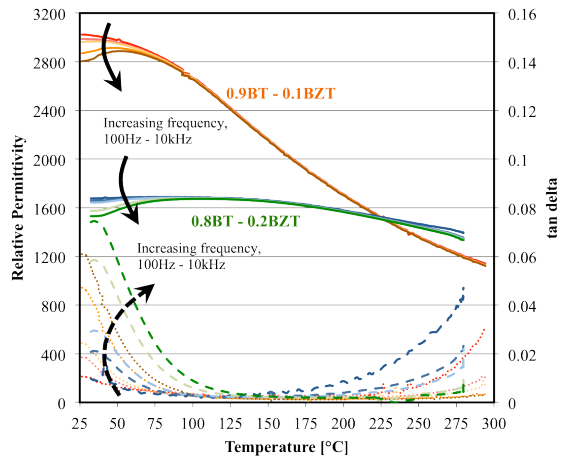


Figure 4 – Temperature- and frequency-dependent small-signal dielectric response of 0.9BT-0.1BZT and 0.8BT-0.2BZT ceramics.

Using a custom high voltage blocking circuit to protect the LCR meter, the small signal (1V ac) dielectric response of ~1mm thick 0.8BT-0.2BZT and 0.9BT-0.1BZT pellets was measured under dc bias supplied by a separate dc power supply. These measurements (not shown) confirmed the stability of the permittivity under large dc bias fields (up to 30kV/cm). Polarization vs. field measurements of both BT-BZT compositions were compared with a commercial high-voltage BST-based capacitor of similar dimensions to our BT-BZT pellets. The BT-BZT pellets were

submersed in fluorinert for the high field measurements. Polarization-Field hysteresis loops resulting from these measurements at 1Hz are shown in Figure 5. The effects of BZT additions are immediately apparent, tilting the hysteresis loop and—in the case of 10% additions, in particular—a thickening of the hysteresis loops. Hysteresis loops were measured at increasing voltages until breakdown. The fully packaged commercial capacitor and the 0.9BT-0.1BZT pellet each broke down through the bulk of the ceramic; the 0.8BT-0.2BZT sample repeatedly arced around the edge of the sample. Interestingly, the packaged commercial capacitor broke down at fields just above 60kV/cm, but both BT-BZT pellets lasted to nearly 100kV/cm. In addition to the decreased voltage tuning that is apparent from the more linear PvSE behavior, this increase in breakdown strength translated into significantly higher stored energy density, as calculated from the PvSE loops in Figure 5 and shown in Figure 6.

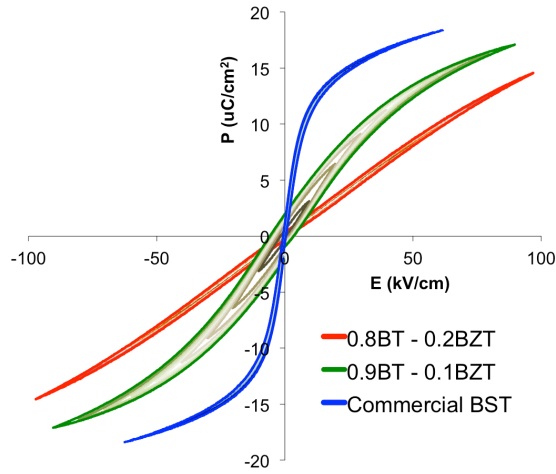


Figure 5 – Polarization vs. Field hysteresis loops measured at 1Hz for BT-BZT pellets as well as a fully-packaged commercial high voltage BST-based capacitor of similar ceramic dimensions for comparison.

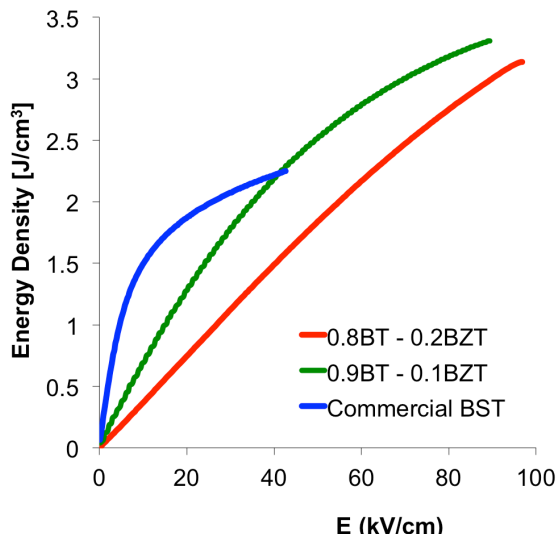


Figure 6 – Energy density available for discharge for BT-BZT pellets of both investigated compositions as well as a commercial BST-based capacitor for comparison.

4. CONCLUSIONS

Initial studies on Bi(Zn,Ti)O₃-modified BaTiO₃ ceramics have confirmed earlier reports of large, minimally-saturating permittivity values. While our samples so far exhibit less frequency-dependent relaxor-like behavior than other reported samples of similar compositions, continued sintering studies are underway to determine the effects of microstructure and cation distribution on the dielectric response. Both the large permittivity and high breakdown strengths lead to significantly larger energy densities than are commonly available for moderately-high voltage (1-10kV) ceramics. Discharged energy densities of greater than 3J/cm³ have already been demonstrated on non-optimized ~1mm thick pellets, an encouraging data point for future investigations into materials in this and related systems.

5. REFERENCES

- [1] J. Sigman, G.L. Brennecke, P.G. Clem, and B.A. Tuttle, *J. Am. Ceram. Soc.*, 91[6], 1851-7 (2008).
- [2] C.-C. Huang, D.P. Cann, X. Tan, and N. Vittayakorn, *J. Appl. Phys.*, 102, 044103 (2007).
- [3] C.-C. Huang and D.P. Cann, *J. Appl. Phys.*, 104, 024117 (2008).
- [4] H. Ogihara, C.A. Randall, and S. Trolier-McKinstry, *J. Am. Ceram. Soc.*, 92[8] 1719-24 (2009).
- [5] Q. Zhang, Z. Li, F. Li, and Z. Xu, *J. Am. Ceram. Soc.*, Early View (Online prior to inclusion in an issue): DOI: 10.1111/j.1551-2916.2011.04695.x (2011).
- [6] T. Strathdee, L. Luisman, A. Feteira, and K. Reichmann, *J. Am. Ceram. Soc.*, 94[8] 2292 (2011).
- [7] M.R. Suchomel and P.K. Davies, *J. Appl. Phys.*, 96[8] 4405-10 (2004).
- [8] R.E. Eitel, C.A. Randall, T.R. Shrout, P.W. Rehig, W. Hackenberger, and S.-E. Park, *Jpn. J. Appl. Phys.*, 40, 5999 (2001).
- [9] R.E. Eitel, S.J. Zhang, T.R. Shrout, C.A. Randall, and I. Levin, *J. Appl. Phys.*, 96[5], 2828-31 (2004).
- [10] O. Khamman, X. Tan, S. Ananta, and R. Yimnirun, *J. Mater. Sci.*, 44, 4321-5 (2009).